Journal of Environmental Health Science and Engineering (2019) 17:753–765
https://doi.org/10.1007/s40201-019-00392-9

RESEARCH ARTICLE

Fixed bed adsorption column studies and models for removal of ibuprofen from aqueous solution by strong adsorbent Nano-clay composite

Lida Rafati[1] · Mohamad Hassan Ehrampoush[1] · Amir Abbas Rafati[2] · Mehdi Mokhtari[1] · Amir Hossein Mahvi[3,4]

Received: 3 September 2018 / Accepted: 3 July 2019 / Published online: 19 July 2019

Abstract
In this study, ibuprofen was removed using a strong nano-clay-composite based on cloisite 15A, PVP and β-cyclodextrin (CD@clay-PVP) adsorbent through a fixed-bed column system. Chemically modified nano-clay was characterized by using Fourier transform infrared spectroscopy (FTIR), scanning electron microscopy (SEM) and XRD. Different input situations were evaluated and included adsorbent bed height, initial concentrations, and the impact of the flow rate on the adsorbent. The various mathematical models employed to predict the breakthrough curve and model parameters include Thomas, bed-depth service time (BDST), Yoon–Nelson, and Clark. The characteristics of parameters related to the models were obtained by linear and nonlinear regression to design the process for the columns. Based on error analysis and adsorption conditions, all of the models are identical in describing the adsorption fixed-bed columns.

Keywords Fixed bed column · Breakthrough models · Adsorption · Ibuprofen · Nano-clay composite

Introduction

Ibuprofen is a non-steroidal anti-inflammatory drug (NSAIDs) used worldwide for treating pain, fever, and inflammation and is on the World Health Organization (WHO) list of essential medicines [1–3]. Developing countries consume several hundred tons of ibuprofen per year. NSAIDs are pharmaceutically active compounds (PhACs), which are a major source of pharmaceutical pollution in the aquatic environment [4, 5]. These drugs cause irreversible changes in the genomes of microorganisms, thereby increasing resistance [6, 7].

✉ Amir Hossein Mahvi
ahmahvi@yahoo.com

[1] Environmental Sciences and Technology Research center, Department of Environmental Health Engineering, Shahid Sadoughi University of Medical Sciences, Yazd, Iran

[2] Department of Physical Chemistry, Faculty of Chemistry, Bu-Ali Sina University, P.O.Box 65174, Hamadan, Iran

[3] Center for Solid Waste Research (CSWR), Institute for Environmental Research (IER), Tehran University of Medical Sciences, Tehran, Iran

[4] Department of Environmental Health Engineering, School of Public Health, Tehran University of Medical Sciences, Tehran, Iran

Epidemiological studies suggest that insufficient evidence available to predict the long-term ramifications of the synergistic and metabolic effects of these pollutants in humans. However, it is already established that their toxic effects in the aquatic environment can adversely impact human health [8, 9]. These compounds are dispersed into sewer systems without modification in stool or urine [6, 7]. Therefore, municipal or domestic wastewater contains a variety of these materials [10, 11]. The manufacturing activities of the pharmaceutical industry release significant amounts of pharmaceutical compounds into the environment (water, soil, and air) [12]. According to Heberer [13], the extent of the occurrence (number of compounds and concentration) of PhACs in water and wastewater has been investigated. The results showed that, in most countries, more than 80 compounds qualifying as PhACs are detectable up to the μg/l-level in aquatic environment. When non-steroidal anti-inflammatory drugs are administered in excessive doses, they result in the formation of toxic metabolites by oxidative pathways and after oxidation they will produce toxins that are relatively unstable in aqueous media and are hydrolyzed into other toxins [6, 11]. Therefore, these drugs must be removed (or, if that is impossible, reduced in terms of concentration) from the aquatic environment. Tertiary or advanced wastewater treatment systems, including micro filtration (MF), nano-filtration

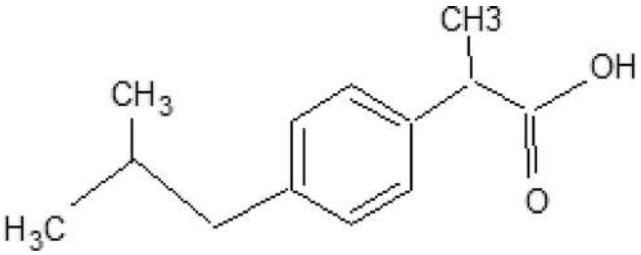

Scheme 1 Structure of ibuprofen is a NSAIDs drug

(NF), reverse osmosis (RO), advanced oxidation processes [14] and adsorption, must be used to remove these drugs from water and wastewater [15–21].

Recently, the trend of using nanostructures and nanocomposites as adsorbents for the removal of pollutants from the environment has been increasing.

Nanoclays contain small and irregular plates of nearly 1 m width and 100 nm diameter. Enclosing a 750 m^2/g of specific surface causes the nanoclays to have manifold efficiencies with a remarkable increase in the features compared with natural clay. Different studies have, as yet, explored the application of clay or nanoclay along with colanders, ceramic filters, clay pipes, or earthen containers. The nanoclays with very small sizes have been of desirable efficiencies in adsorption of both organic and heavy metals [22]. Clay minerals have also been widely used as adsorbents due to their low-cost, natural abundance, and environmental friendliness. The cost of clays (0.04–0.12 US \$ kg^{-1}) are up to 20 times more cheaper than activated carbon (20–22.00 US \$ kg^{-1}) [23]. In addition, clays exhibit a moderate specific surface area [23, 24] and a high cation exchange capacity [25].

In this study, a strong nano-clay-composite adsorbent was used to remove ibuprofen from an aqueous solution. The aim of this study is to investigate the effect of a new nano-clay-composite for the removal of ibuprofen as measured by different parameters including column bed height, initial concentration, and flow rate. Finally, the fixed-bed column adsorption models were analyzed using multiple mathematical models (Thomas, bed-depth service time (BDST), Clark, Yoon–Nelson).

Materials and methods

Chemical material

Closite 15 A was purchased from Neutrino Co. (Iran), β-Cyclodextrine from Merck (Germany), 3-aminopropyl triethoxysilane (APTS) and p-toluenesulfonyl chloride (TsCl) from Sigma-Aldrich and all the other reagents were analytical grade and used without further purification. Ibuprofen with high purity was gift from Tehran Daru (Iranian pharmaceutical company). The amount of ibuprofen in each stage was measured using a UV-Vis spectrophotometer (PG-Instruments Ltd.) at 225 nm [26] (Scheme 1 shows the chemical structure of ibuprofen).

Preparation of adsorbent

Clay/β-CD/PVP nano-composite adsorbent (*CCP*) was synthesized according to using Tan et al. method [27] with slight

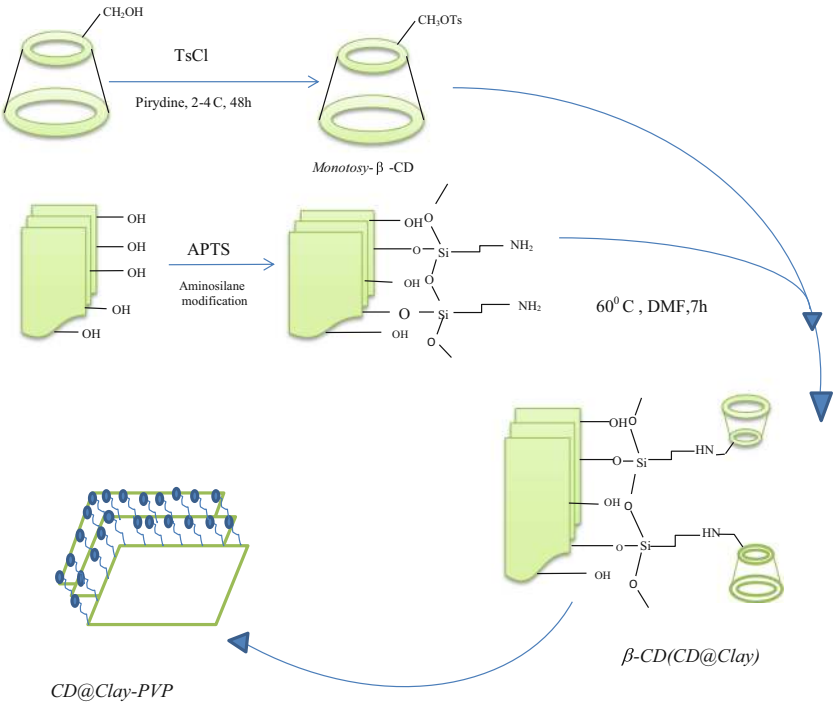

Scheme 2 Schematic procedure for synthesis of CCP

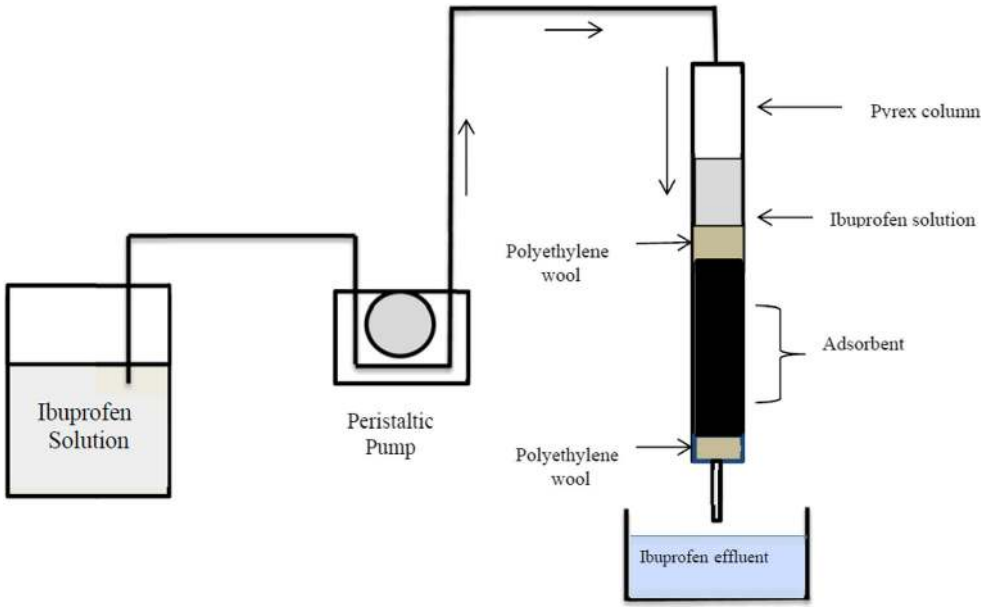

Scheme 3 Schematic of continues fixed bed column process

modification. Briefly, a Solution β-CD was vigorously stirred by adding 18 g of β-CD (16 mmol) to 100 ml of dry pyridine in order for the β-CD to dissolve completely. Next, 2.5 g of toluenesulfonyl chloride (12 mmol) was added to it. The

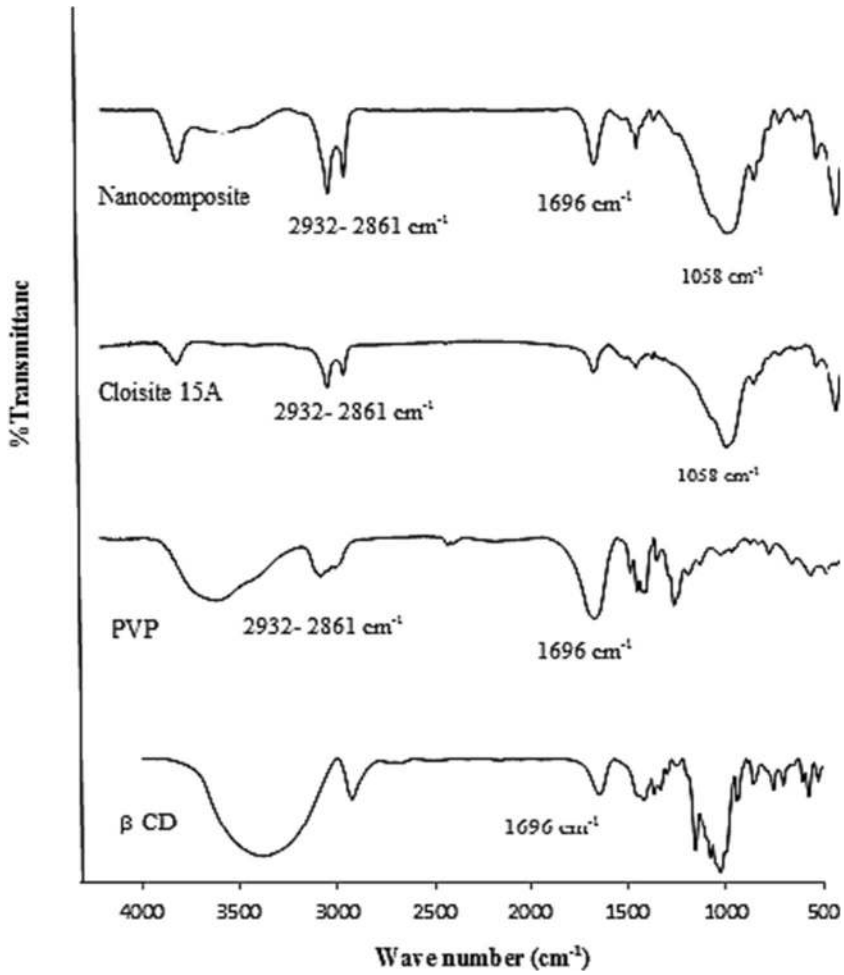

Fig. 1 The FT-IR spectra of the cyclodextrin, PVP, cloisite 15A and CCP

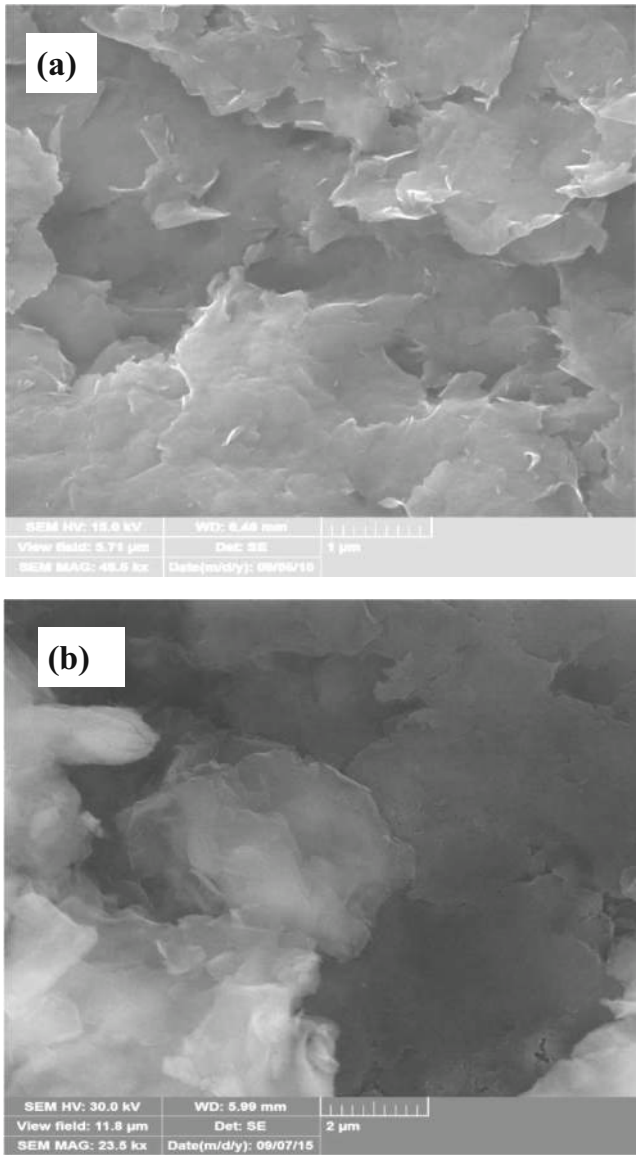

Fig. 2 SEM images of (**a**) Closite 15A and (**b**) CCP nanocomposite

reaction was then refluxed for 8 h at 2–4 °C and kept at room temperature for 2 days. This solution was concentrated under vacuum conditions and then poured into diethyl ether. Then it was centrifuged and drained with distilled water several times. It was then placed inside an oven under vacuum condition at 60 °C. The obtained solution was in the form of a white precipitate which was then collected.

For grafting of clay with β-CD, 50 ml of dimethyl formamide (DMF) together with 2 g of Cloisite 15A were refluxed inside a three-neck flask equipped with a condenser at room temperature. Then, 0.25 g of β-CD-OTs was added to 10 ml of DMF and mixed with the initial mixture at pH = 7–8. The temperature was then increased to 60 °C and next the reaction was stirred by a magnetic stirrer for 7 h under nitrogen atmosphere. The obtained product was next filtered and washed by DMF and acetone for removing unreacted compounds. In order to remove the residual solvent, it was dried inside a drying cabinet for 24 h at 60 °C.

Following grafting, intercalation was done between the layers by polyvinylpyrrolidone (PVP). A suspension of 0.5 g of grafted clay with β-CD in 15 ml of toluene was added dropwise to a solution of containing 0.05 g of PVP and 15 ml of toluene through ultra-sonication for 1 h. The obtained product was exposed to room temperature for one day, then centrifuged and washed with toluene three times, and eventually dried at 60 °C for overnight (Scheme 2).

Fixed –bed column experiments

The pilot of fixed bed column was presented in Scheme 3. Fixed- bed column with an inner diameter of 1 cm and 30 cm in height were made of glass Pyrex. In order to avoid the withdrawal of adsorbent column, the Column was fixed by polyethylene wool. It was necessary to set up a certain amount of adsorbent used in the column of nano-adsorbent clay. Several distilled water was passed to adsorbent packed in the column in order to the removal of air trapped between adsorbent particles. Then, ibuprofen solutions were continuously fed downward into the column and the samples were collected at different time and were analyzed by UV-Vis spectrophotometer.

Effect of bed height

In order to measure effect of the bed height, nano adsorbent clay was used in different amounts and was used in separate columns. Adsorbent bed height was measured in columns 1.5, 2 and 2.5 cm, respectively. The initial solution of ibuprofen with concentration of 3 mg/l was evaluated and was passed separately to the column with a flow rate of 6 ml/min and empty bed contact time (EBCT) =1.96 min. Effluent samples of the column were collected and were analyzed.

Effect of flow rate

The effect of ibuprofen influent flow rate into the column, at flow rates of 6 and 9 ml/min was measured with the initial concentration of 3 mg/l, EBCT = 1.96 min and the adsorbent rate of 1 g (bed height of 1.5 cm). At the end of the column, samples were collected for analysis.

Effect of initial concentration

Ibuprofen stock solution was prepared and the concentrations of 3, 5 and 10 mg/l were prepared from it. The performance of fixed-bed column was measured for different input concentration of ibuprofen at Q = 6 ml/min, EBCT = 1.96 min, and adsorbent rate of 1 g (bed height of 1.5 cm). Each

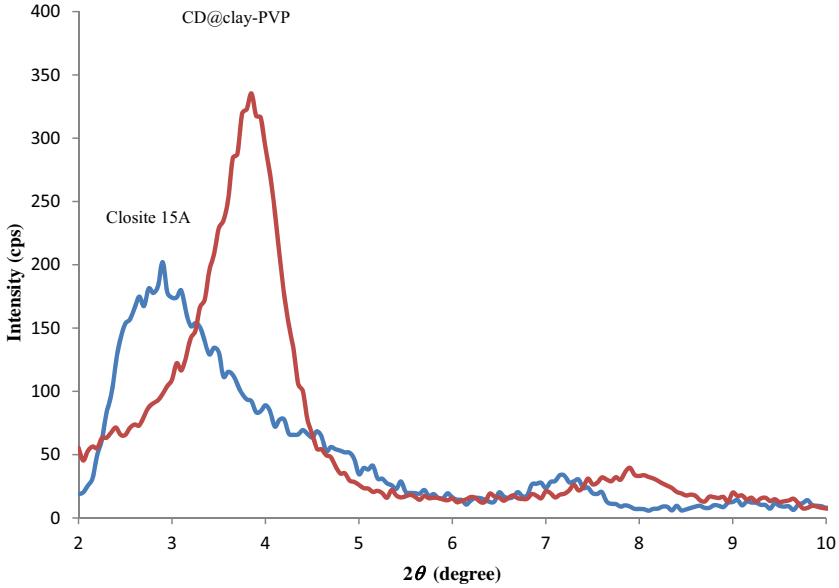

Fig. 3 XRD patterns of Closite 15A and CCP nanocomposite

concentration was established separately and at the end of the column the samples were collected and kept for analysis.

Theoretical description of fixed bed column studies

The column behavior for adsorption of ibuprofen is expressed as C_{eff}/C_0 (C_{eff} and C_0 are the concentration of column-effluent ibuprofen and the initial concentration of column-influent ibuprofen, respectively) against the flow time and is accordingly plotted on the breakthrough curve [28]. Breakthrough time and the shape of breakthrough curve are major factors that can effectively be used to determine the efficiency of the adsorption column. The velocity and concentration of the adsorbate are the factors involved in the shape a fixed-bed column. The total adsorbed ibuprofen, q_{tot} (mg), in the column for inlet concentration of C_0 and the flow rate Q (ml/min) are obtained by integrating the plot of adsorbed concentration (C_{ad}) versus the flow time according to Eq. (1):

$$q_{tot}(mg) = \frac{QA}{1000} = \frac{Q}{1000}\int_{t=0}^{t=t_{tot}} C_{ad}dt \tag{1}$$

The total amount of ibuprofen delivered to the column system m_{tot} (mg) is calculated from Eq. (2) [29]:

$$m_{\text{tot}}(\text{mg}) = \frac{C_0 V_{\text{eff}}}{1000} \tag{2}$$

In this equation C_o and C_t are the initial concentration of ibuprofen and adsorbed concentration at time (t) respectively and C_{ad} is equal to C_{o}-C_{t} and V_{eff} is the output volume of the column. Equilibrium adsorption capacity q_e (mg/g) from the rate of adsorbed ibuprofen per gram of adsorbent is calculated according to Eq. (3):

$$q_{e\ (\text{mg/g})} = \frac{q_{tot}}{M} \tag{3}$$

M is the gram of adsorbent was used in the fixed-bed column. The removal percentage of ibuprofen as follow as Eq. (4):

$$R(\%) = \frac{q_{tot}}{m_{tot}} \times 100 \tag{4}$$

Table 1 Parameters in fixed-bed column for ibuprofen adsorption

Parameters	C_0 (mg/l)	Q(ml/min)	H_{T} (cm)	t_{tot} (min)	m_{tot} (mg)	q_{tot} (mg)	q_{e} (mg/g)	$V_{\text{eff (ml)}}$	R (%)	EBCT (min)
Bed height	3	6	1.5	400.00	7.20	3.780	3.78	2400	52.50	1.96
	3	6	2.0	433.33	7.80	5.295	3.53	2600	67.88	1.96
	3	6	2.5	458.33	8.25	6.920	3.46	2750	83.87	1.96
Concentration	3	6	1.5	400.00	7.20	3.780	3.78	2400	52.50	1.96
	5	6	1.5	333.33	10.00	6.17	6.17	2000	61.70	1.96
	10	6	1.5	308.33	18.5	12.55	12.55	1850	67.83	1.96
Flow rate	3	6	1.5	400.00	7.20	3.780	3.78	2400	52.50	1.96
	3	9	1.5	200.00	5.4	2.82	2.82	1800	52.22	1.30

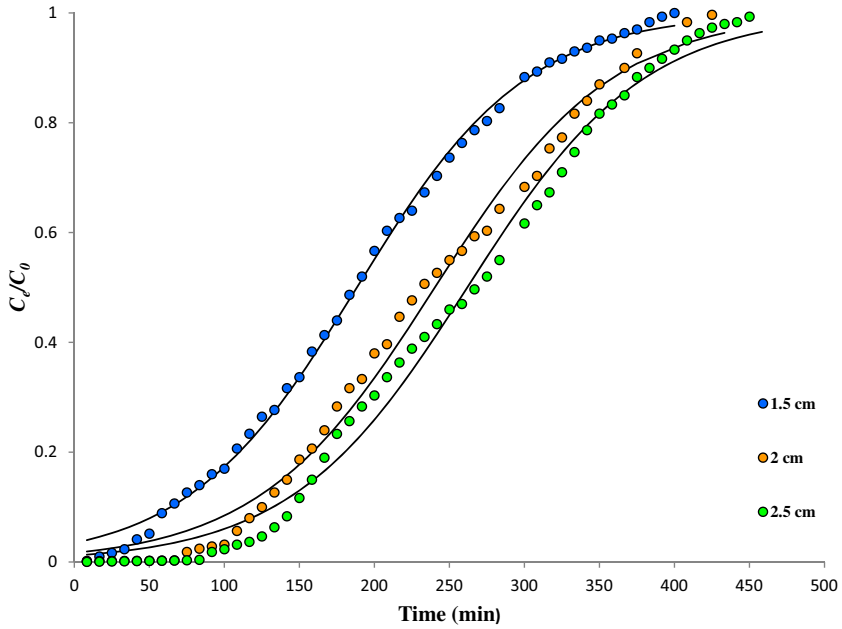

Fig. 4 Effect of different bed heights on the breakthrough curve of ibuprofen. Experimental and predicted breakthrough curve data is indicated by circles and lines, respectively

Results and discussion

Characterization of CCP adsorbent

Scheme 2 represents the overall procedure used for synthesis of nano-composite functionalized with β-CD. The FT-IR spectra related to (a), β-CD (b), PVP (c) Cloisite 15A and (d) *CCP* are shown in Fig. 1. IR spectra nano-composite (CCP) showed nano-composite bands that can be detected on β-CD, PVP, and Cloisite 15A spectra. For example, the band emerged at 1058 cm^{-1} for cloisite 15A (Si—O stretching vibration) does not exist on β-CD and PVP spectrum, but it was present on the nano-composite spectrum. The silylated Cloisite 15A clay had specific peaks at 1058 529, and 467 cm^{-1} resulting from Si—O group. The bands present at 1969 cm^{-1} (C=O stretching vibration) on PVP do not exist on clay and β-CD, but were presented on the nano-composite. Further, clay had IR peak at 3645 cm^{-1} corresponding to the O—H free group. The Peaks at 2932 and 2861 cm^{-1} are a result of organic modifier alkyl chains in the clay. Meanwhile, the nano-composite has the following IR peaks: Si—O (1058, 529, and 467 cm^{-1}) and CH_2 (2932, 2861 cm^{-1}) peaks associated with polymer and clay, respectively.

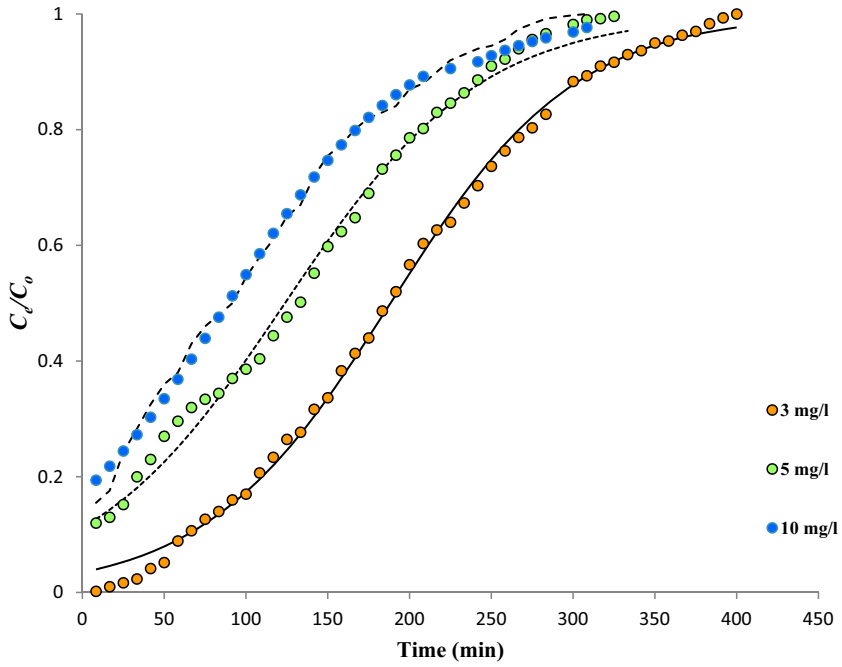

Fig. 5 Effect of different concentrations on the breakthrough curve of ibuprofen. Experimental and predicted breakthrough curve data is indicated by circles and lines, respectively

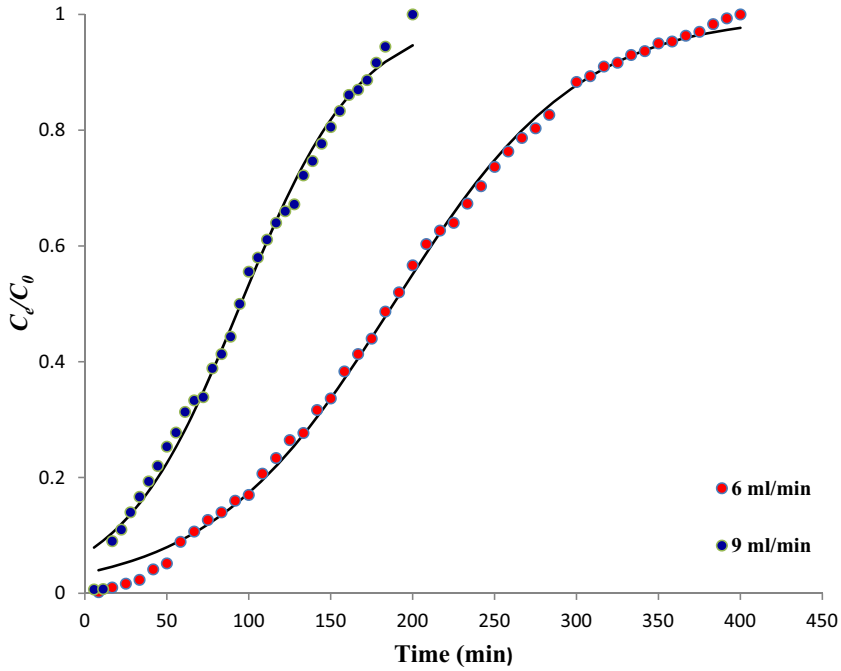

Fig. 6 Effect of different flow rates on the breakthrough curve of ibuprofen. Experimental and predicted breakthrough curve data is indicated by circles and lines, respectively

The SEM method was used for investigating the surface morphologies of the prepared samples. The surface morphology of the clay nano-powder and functionalized clay nano-composite fabricated by PVP (CCP) are shown in Fig. 2. The SEM images related to the fabricated nano-composite (CCP) in Fig. 2b indicates different surface morphologies when compared with surface morphologies of clay nano-powder (Fig. 2a). It is observed that the spaces of the internal layers have grown in Fig. 2b, suggesting saturation of polymer nanoparticles between clay layers.

XRD patterns of clay nano-powder and clay nano-composite with PVP are revealed in Fig. 3. The specific characteristics of these patterns include: (a) clay nano-powder has a peak at $2\theta = 7.3°$, corresponding to the crystallographic plane (001) of its crystal structure, with the Layer distance of clay being around 1.21 nm. (b) A peak at $2\theta = 2.9°$ which corresponds to the MMT distance layer of 3.04 nm. In comparison with cloisite 15A, CCP represents higher interlayer distances suggesting that the polymer has successfully penetrated into MMT's layers.

The CCP composite indicated a variation in peak towards a lower refraction angle (2θ) of the pure cloisite 15A, suggesting increased interlayer space of silicate layers and diffusion of polymer chains between clay layers. The reduction in the peak intensity is attributed to the lower amount of clay in the composite relative to the pure nano-clay. Various researchers have reported altered peaks from a higher refraction angle to lower angles [30, 31].

Fixed bed column studies

The fixed bed column system is expressed by breakthrough curve. The behavior of column for adsorption of ibuprofen is provided as C_{eff}/C_0 against the flow time (t). Then, by using mathematical theories of the column system, the data obtained were applied. The total removal of column ibuprofen and related parameters are presented in Table 1.

Effect of bed height

Breakthrough curves of ibuprofen adsorption on the adsorbent at different bed heights (1.5, 2 and 2.5 cm) were evaluated (flow rate = mL min^{-1}, EBCT = 1.96 min and influent ibuprofen concentration = mg L^{-1}) (Fig. 4). According to Fig. 4, the breakthrough time was increased by increasing the bed height. Table 1 represents the parameters in fixed-bed column for ibuprofen adsorption by adsorbent. As shown in Table 1, bed height strongly influenced on the adsorption of the ibuprofen uptake capacity of 3.78, 3.53 and 3.46 mg/g, was obtained at 1.5, 2 and 2.5 cm, respectively. Also, the results showed that the breakthrough time increased from 400 min to 458 min, with increasing bed height from 1.5 to 2.5 cm.

Table 2 Predicting adsorption models for Breakthrough curve

Breakthrough curve Model	Equation
BDST	$t = \left(\frac{N_0\ HT}{c_0\ U}\right) - \left(\frac{1}{k_0\ c_0}\right)\ ln\left(\frac{c_0}{c_t} - 1\right)$ (5)
Thomas	$\ln\left(\frac{c_0}{c_t} - 1\right) = \left(\frac{k_{Th} q_0 M}{Q}\right) - \left(\frac{k_{Th} c_0 V_{eff}}{Q}\right)$ (6)
Yoon –Nelson	$\ln\frac{c_t}{c_0 - c_t} = k_{YN} t - \tau k_{YN}$ (7)
Clark	$\frac{c}{c_0} = \left(\frac{1}{1 + Ae^{-rt}}\right)^{\frac{1}{n-1}}$ (8)

Table 3 BDST parameters at different conditions for the adsorption of ibuprofen

Parameters	C_0 (mg/L)	H_T (cm)	Q (mL/min)	k_0 (L mg^{-1} min^{-1})	N_0 (mg L^{-1})	U (cm min^{-1})	R^2
Bed height	3	1.5	6	0.005625	2328.624	6.18	0.9980
	3	2.0	6	0.006084	2125.332	6.18	0.9929
	3	2.5	6	0.006553	1788.294	6.18	0.9653
Concentration	3	1.5	6	0.005625	2328.624	6.18	0.9980
	5	1.5	6	0.003609	2969.966	6.18	0.9974
	10	1.5	6	0.001719	3682.868	6.18	0.9941
Flow rate	3	1.5	6	0.005625	2328.624	6.18	0.9980
	3	1.5	9	0.00083	1536.541	8.08	0.9920

When the bed height of the adsorbent was increased, binding sites were provided for the attachment of ibuprofen molecules for adsorption [32]. Also, with the bed height increased, effluent volume (V_{eff}) is increased that due to the more contact time [33]. The slope of the breakthrough curve was reduced based on the increasing bed height due to the expansion of the mass-transfer zone [34–36].

Effect of initial concentration

Function of adsorption column was investigated for various input concentrations of ibuprofen (3, 5 and 10 mg/l) in flow rate of 6 ml/min and bed height of 1.5 cm. Equilibrium uptake of ibuprofen was increased with increasing initial concentrations (Table 1). Breakthrough time decreased by increasing the initial concentration of ibuprofen according to data presented in Table 1 and Fig. 5 due to rapid saturation of bed, since adsorbent particles are exposed to higher levels of adsorbed materials; sharper breakthrough curves were observed with increasing concentration, indicating smaller mass transfer zone and higher adsorption rate [37].

Effect of flow rate

The effect of flow rate of flow rates on the breakthrough curves were studied by flow rates of 6 and 9 ml/min. The breakthrough curves at different flow rates of ibuprofen are presented in Fig. 6. As shown in Fig. 6, with the flow rate increased the breakthrough curve became faster. In all cases, a feed solution having an initial ibuprofen concentration of 3 mg/L was passed through a fixed bed of depth 1.5 cm. As the flow rate was increased from 6 to 9 mL/min, the EBCT decreased from 1.96 to 1.3 min and the breakthrough time was decreased from 400 to 200 min (Table 1).

With increasing flow rates decreasing the breakthrough time because the adsorbent is saturated and ions have a lower level of contact time with adsorbent. The amount of total ibuprofen uptake (q_e) decreased from 3.78 to 2.82 mg/g as flow rate increased from 6 to 9 mL/min.

Adsorption modeling

Prediction of the breakthrough curve for the effluent need to design of a column adsorption process [38]. In order to

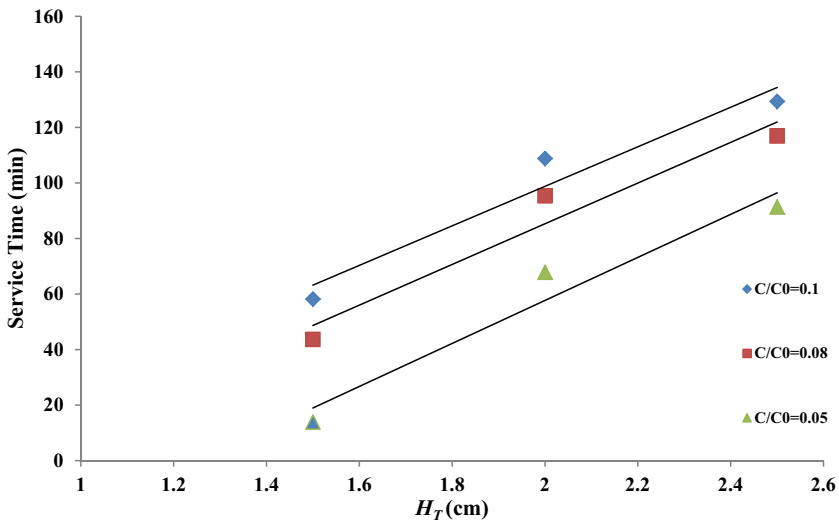

Fig. 7 Times of breakthroughs with respect to bed height according to the BDST model

Table 4 Regression analysis of service time versus bed height for determination of the minimum bed height corresponding to time $t = 0$ (H_0)

C/C_0	Regression equation	N_0	k_0	H_0	R^2
0.05	$t = 77.45\ H_T - 97.192$	1435.923	0.02260	1.2549	0.9511
0.08	$t = 73.236\ H_T - 68.158$	1357.795	0.03993	0.8350	0.9465
0.10	$t = 71.179\ H_T - 43.566$	1319.659	0.06758	0.6120	0.9439

Table 5 Thomas model parameters at different conditions for the adsorption of ibuprofen

Parameters	C_0 (mg/L)	H_T (cm)	Q (mL/min)	k_{Th} (mL/min mg)	q_0 (mg/g)	R^2
Bed height	3	1.5	6	5.60	2.330	0.9977
	3	2.0	6	4.60	2.830	0.9840
	3	2.5	6	4.40	3.340	0.9740
Concentration	3	1.5	6	5.60	2.330	0.9977
	5	1.5	6	3.840	3.936	0.9963
	10	1.5	6	1.740	5.497	0.9939
Flow rate	3	1.5	6	5.60	2.330	0.9977
	3	1.5	9	8.40	1.561	0.9963

Table 6 Yoon–Nelson parameters at different conditions for the adsorption of ibuprofen

Parameters	C_0 (mg/L)	H_T (cm)	Q (mL/min)	k_{YN} (min^{-1})	τ (min)	R^2
Bed height	3	1.5	6	0.0166	187.95	0.9985
	3	2.0	6	0.0150	236.53	0.9849
	3	2.5	6	0.0149	266.33	0.991
Concentration	3	1.5	6	0.0166	187.95	0.9985
	5	1.5	6	0.0176	128.55	0.9962
	10	1.5	6	0.0180	91.93	0.9929
Flow rate	3	1.5	6	0.0166	187.95	0.9985
	3	1.5	9	0.0262	95.03	0.9965

Table 7 Clark parameters at different conditions for the adsorption of ibuprofen

Parameters	C_0 (mg/L)	H_T (cm)	Q (mL/min)	r	A	R^2
Bed height	3	1.5	6	0.0137	4.0548	0.9980
	3	2.0	6	0.0125	5.954	0.9901
	3	2.5	6	0.0117	6.405	0.9803
Concentration	3	1.5	6	0.0137	4.0548	0.9980
	5	1.5	6	0.0151	2.1662	0.9922
	10	1.5	6	0.0171	1.6482	0.9927
Flow rate	3	1.5	6	0.0137	4.0548	0.9980
	3	1.5	9	0.0203	2.1357	0.9958

Table 8 Equations for error functions for fixed bed column study

Error functions	Equation
Residual root mean square error (*RMSE*)	$\mathrm{RMSE} = \sqrt{\frac{1}{n-2}\sum_{i=1}^{n}\left(Y_{exp}-Y_{cal}\right)^2}$
The coefficient of determination (R^2)	$R^2 = \frac{\left(Y_{exp}-\overline{Y_{cal}}\right)^2}{\sum_{i=1}^{n}\left(Y_{exp}-\overline{Y_{cal}}\right)^2+\left(Y_{exp}-Y_{cal}\right)^2}$
The sum of the square of the error (*SSE*)	$SSE = \sum_{i=1}^{n}\left(Y_{exp}-Y_{cal}\right)^2$
The sum of the absolute error (*SAE*)	$SAE = \sum_{i=1}^{n}\left\lvert Y_{cal}-Y_{exp}\right\rvert_i$
Average relative error (*ARE*)	$ARE = \frac{1}{n}\sum_{i=1}^{n}\left\lvert\frac{Y_{cal}-Y_{exp}}{Y_{exp}}\right\rvert$
The average relative standard error (*ARS*)	$\mathrm{ARS} = \sqrt{\frac{\sum_{i=1}^{n}\left(Y_{cal}-Y_{exp}/Y_{exp}\right)^2}{n-1}}$

describing and analyzing the fixed bed column studies several theoretical models have been investigated [39, 40]. In this study, BDST, Thomas, Yoon- Nelson and Clark models were applied for predicting the dynamic behavior of the column. Some of these equation models are listed in Table 2.

BDST (bed depth service time) model analysis

BDST is a simplified model of Bohart-Adams with linear relationship between the bed depth and service time. This model was developed by Hutchin and introduced as BDST (Eq. 5) [41]. This model is having different modes of bed depth, H_T, service time in the column. N_o and k_o constants were obtained during column operation and R^2 shows the compliance of adsorption system from BDST. A suitable correlation for all plots ($R^2 >$ 0.97) is indicative of high applicability of the model to predict the service time of the adsorbents used in the column (Table 3). k_o was obtained through BDST plots, indicating the properties of solute transfer levels from liquid phase to solid phase [42].

BDST model parameters can be useful to scale up the process in other flow rates without testing. The minimum bed height corresponding to time $t = 0$ may be predicted from the plot (Fig. 7). The minimum bed heights were estimated and presented in Table 4 for different C_t/C_0.

Thomas model

The Thomas model is presented in a linearized form, in Eq. (6). Based on Thomas model, Thomas kinetic coefficient (K_{Th}) and Maximum solid phase concentration (mg/g) are respectively calculated through slope and intercept of linearized plots form and the behavior is described in the column [43]. K_{Th} and q_0 values increased with increasing bed height (Table 5). On the other hand, K_{Th} was increased from 5.6 to 8.4 $\mathrm{mLmin^{-1}\ mg^{-1}}$ by increasing the flow rate and q_0 was decreased from 2.33 to 1.561 $\mathrm{mg\ g^{-1}}$. The results showed that lower flow rate and higher bed height lead to better adsorption of ibuprofen on adsorbent.

Yoon-Nelson model

The simple theoretical Yoon–Nelson model, suitable for single component system, was tested to predict the behavior of breakthrough for ibuprofen on adsorbent [44]. The linearized Yoon–Nelson model is expressed in Eq. (7). k_{YN} is the rate constant ($\mathrm{min^{-1}}$) and τ is the time required for 50% exchange breakthrough (min). The values of k_{YN} and τ wrer determined by plotting ln $[C_t/(C_0 - C_t)]$ versus t. Calculated parameters of (t value at 50% breakthrough), k_{YN} (a rate constant) and other

Table 9 Error functions for prediction of breakthrough curve at various bed column conditions for all models

Parameters	C_0 (mg/l)	Q(ml/min)	H_T (cm)	R^2	*RMSE*	*SSE*	*SAE*	*ARE*	*ARS*
Bed height	3	6	1.5	0.9989	0.0162	0.0119	0.5669	0.602	2.868
	3	6	2.0	0.9954	0.0329	0.0481	1.3368	2.761	6.231
	3	6	2.5	0.9963	0.0317	0.0527	1.5287	3.212	7.952
Concentration	3	6	1.5	0.9989	0.0162	0.0119	0.5669	0.602	2.868
	5	6	1.5	0.9966	0.0242	0.0219	0.7714	0.0450	0.0625
	10	6	1.5	0.9980	0.0167	0.0138	0.5736	0.0357	0.0662
Flow rate	3	6	1.5	0.9989	0.0162	0.0119	0.5669	0.602	2.868
	3	9	1.5	0.9957	0.0285	0.0268	0.7042	0.6752	2.698

Table 10 Comparison of our developed nano composite adsorbent performance with some reported adsorbents

Adsorbate	Adsorbent	% Removal	Reference
Anti-inflammatory drugs (NSAIDs)	natural clay	7.04%	Khazri et al. (2016)
	molecularly imprinted polymer (MIP)	69%	Madikizela and Chimuka (2016)
	Octolig®	80%	Martin et al. (2016)
	Olive waste cakes	70.07%	Baccar et al. (2012)
	functionalized nano-clay composite	94.5%	The present study

statistical parameters for different situations of input concentrations of ibuprofen, bed height and flow rate have been presented in Table 6. k_{YN} value decreased by increasing bed height and input concentrations of ibuprofen because of rapid saturation of column and elevated due to increasing flow rate. Correlation coefficients related to experimental and predictable data using Yoon–Nelson model in all phases were 0.991 and 0.9985, respectively.

Clark model

Clark model is expressed in Eq. 8. A and r parameters were calculated based on linear equation of Clarke model [45]. Table 7 indicates the value of these parameters for different modes of input concentrations of ibuprofen, bed height and flow rate. Value of A decreased by increasing initial concentration and flow rate and showed an increase by elevating bed height, but the ratio of r was in contrast [46–50]. R^2 in 0.9901 and 0.9980 range indicates that the model is suitable for predicting the breakthrough curve of ibuprofen uptake process as well as is simulated model of Freundlich adsorption kinetic.

Comparison between applied models

Data analysis using error analysis is required to confirm the adsorption system models. Equations for error functions are listed in Table 8. The experimental data was very consistent with the curve fitting obtained from the models, confirming the control of external mass transfer by initial breakthrough curves. The column adsorption models used in this study to fit the ibuprofen adsorption data can be essentially grouped based on these equations. The characteristics of the parameters associated with these models were different, but all four models predicted a substantial amount of C_t/C_0 for a particular set of data. The unique properties related to parameters of error functions presented in Table 9 created more possibilities for comparison.

According to the results obtained by the error analysis include R^2, and other statistical parameters such as residual root mean square error (RMSE), the sum of the square of the error (SSE), the sum of the absolute error (SAE), average relative error (ARE) and the average relative standard error (ARS) can be easily concluded that these four models are essentially the same as each other. Thus, the overlap of all the data points is clear based on the results of the simulation, and the effective parameters for measuring the functioning of the fixed-bed column suggested the usefulness of the models.

Conclusions

In this study, we synthesized a Clay/β-CD/PVP *(CCP)* nanocomposite adsorbent to remove ibuprofen from aqueous solutions and examined the efficiency of this adsorbent through fixed-bed column studies. Parameters affecting the function of the column, such as bed heights, flow rates, and initial ibuprofen concentrations, were studied with respect to adsorption capacity and breakthrough curve profiles. The results show that adsorption capacity was increased with increasing concentrations and the bed depth and decreased with increases in flow rate. The Thomas, BDST, Yoon–Nelson, and Clark mathematical models were analyzed to predict the breakthrough curves and characterize the ibuprofen adsorption parameters for the nano-composite adsorbent in different situations. The relevant characteristics of these models were measured by adopting non-linear regression, indicating appropriate fitting of experimental data due to bed heights, flow rates, and initial ibuprofen concentration values. Compared to other studies (Table 10), the adsorbent presented in this study had better adsorption capacity.

Acknowledgements This research has been technically and financially supported by Shahid Sadoughi University of Medical Sciences.

References

1. Petrie B, Barden R, Kasprzyk-Hordern B. A review on emerging contaminants in wastewaters and the environment: current knowledge, understudied areas and recommendations for future monitoring. Water Res. 2014;72:1–27.
2. Mestre AS, Pires J, Nogueira JMF, Parra JB, Carvalho AP, Ania CO. Waste-derived activated carbons for removal of ibuprofen from solution: role of surface chemistry and pore structure. Bioresour Technol. 2009;100:1720–6.
3. Heckmann LH, Helen AC, Hooper L, Connon R, Hutchinson TH, Maund SJ, et al. Chronic toxicity of ibuprofen to Daphnia magna:

effects on life history traits and population dynamics. Toxicol Lett. 2007;172:137–45.
4. Daughton CG, Ternes TA. Pharmaceuticals and personal care products in the environment: agents of subtle change? Environ Health Perspect. 1999;107:907–38.
5. Grote M, Haciosmanoglu B, Bataineh M, Nolte J. Separation of drug traces from water with particular membrane systems. J. Environ. Sci. Health a: toxic Hazard. Subst. Environ. Eng. 2004;39:1039–53.
6. Bagheri A, Mahvi AH, Nabizadeh R, Dehghani MH, Mahmoudi B, Akbari-Adergani B, et al. Rapid destruction of the non-steroidal anti-inflammatory drug diclofenac using advanced Nano-Fenton process in aqueous solution. Medica. 2017;5:879.
7. Esplugas S, Bila DM, Krause LGT, Dezotti M. Ozonation and advanced oxidation technologies to remove endocrine disrupting chemicals (EDCs) and pharmaceuticals and personal care products (PPCPs) in water effluents. J Hazard Mater. 2007;149:631–42.
8. Le MS, Bot B, Thomas O. Occurrence and fate of pharmaceutical products and by-products, from resource to drinking water. Environ Int. 2009;35:803–14.
9. Santos JL, Aparicio I, Callejón M, Alonso E. Occurrence of pharmaceutically active compounds during 1-year period in wastewaters from four wastewater treatment plants in Seville (Spain). J Hazard Mater. 2009;164:1509–16.
10. Jayasiri HB, Purushothaman CS, Vennila A. Pharmaceutically active compounds (PhACs): a threat for aquatic environment? J Marine Sci Res Dev. 2013;4:e122. https://doi.org/10.4172/2155-9910.1000e122.
11. Carballa M, Omil F, Lema JM, Llompart M. García-Jares C. Rodríguez I. Gómez M. Ternes T. behavior of pharmaceuticals, cosmetics and hormones in a sewage treatment plant. Water Res. 2004;38:2918–26.
12. Vogelsang C, Grung M, Jantsch TG, Tollefsen KE, Liltved H. Occurrence and removal of selected organic micropolluants at mechanical, chemical and advanced wastewater treatment plants in Norway. Water Res. 2006;40:3559–70.
13. Heberer T. Occurrence, fate, and removal of pharmaceutical residues in the aquatic environment: a review of recent research data. Toxicol Lett. 2002;131:5–17.
14. Urtiaga AM, Pérez G, Ibáñez R, Ortiz I. Removal of pharmaceuticals from a WWTP secondary effluent by ultrafiltration/reverse osmosis followed by electrochemical oxidation of the RO concentrate. Desalination. 2013;331:26–34.
15. Kamranifar M, Naghizadeh A. Montmorillonite nanoparticles in removal of textile dyes from aqueous solutions: study of kinetics and thermodynamics. Iranian Journal of Chemistry and Chemical Engineering (IJCCE). 2017;36:127–37.
16. Nasseri S, Mahvi AH, Yaghmaeian K, Nabizadeh R, Alimohammadi M, Safari GH. Degradation kinetics of tetracycline in aqueous solutions using peroxydisulfate activated by ultrasound irradiation: effect of radical scavenger and water matrix. J Mol Liq. 2017;241:704–14.
17. Safari GH, Nasseri S, Mahvi AH, Yaghmaeian K, Nabizadeh R, Alimohammadi M. Optimization of sonochemical degradation of tetracycline in aqueous solution using sono-activated persulfate process. J Environ Health Sci Eng. 2015;13:76.
18. Khodadadi M, Ehrampoush MH, Ghaneian MT, Allahresani A, Mahvi AH. Synthesis and characterizations of FeNi3@SiO2@TiO2 nanocomposite and its application in photocatalytic degradation of tetracycline in simulated wastewater. J Mol Liq. 2018;255:224–32.
19. Rostamian R, Najafi M, Rafati AA. Synthesis and characterization of thiol-functionalized silica nano hollow sphere as a novel adsorbent for removal of poisonous heavy metal ions from water: kinetics, isotherms and error analysis. Chem Eng J. 2011;171:1004–11.
20. Najafi M, Rostamian R, Rafati AA. Chemically modified silica gel with thiol group as an adsorbent for retention of some toxic soft metal ions from water and industrial effluent. Chem Eng J. 2011;168:426–32.
21. Nadeali A, Khoobi M, Nabizade R, Nasseri S, Mahvi AH. Performance evaluation of montmorillonite and modified montmorillonite by polyethyleneimine in removing arsenic from water resources. Desalin Water Treat. 2016;57:21645–53.
22. Pandey S. A comprehensive review on recent developments in bentonite-based materials used as adsorbents for wastewater treatment. J Mol Liq. 2017;241:1091–113.
23. Bhattacharyya KG, Gupta SS. Adsorption of a few heavy metals on natural and modified kaolinite and montmorillonite: a review. Adv Colloid Interf Sci. 2008;140:114–31.
24. Long H, Wu P, Zhu N. Evaluation of Cs+ removal from aqueous solution by adsorption on ethylamine-modified montmorillonite. Chem Eng J. 2013;225:237–44.
25. He H, Ma Y, Zhu J, Yuan P, Qing Y. Organoclays prepared from montmorillonites with different cation exchange capacity and surfactant configuration. Appl Clay Sci. 2010;48:67–72.
26. Zhou Z, Jiang JQ. Detection of ibuprofen and ciprofloxacin by solid-phase extraction and UV/Vis spectroscopy. J Appl Spectrosc. 2010;79:459–64.
27. Tan T, Ng SC, Wang Y, Xiao Y. Synthesis of mono-6-tosyl-β-cyclodextrin, a key intermediate for the functional cyclodextrin derivatives. Protoc exch. 2011;6:935–42.
28. Guibal E, Lorenzelli R, Vincent T, Cloirec PL. Application of silica gel to metal ion sorption: static and dynamic removal of uranyl ions. Environ Technol. 1995;16:101–14.
29. Wang W, Li M, Zeng Q. Adsorption of chromium (VI) by strong alkaline anion exchange fiber in a fixed-bed column: experiments and models fitting and evaluating. Sep Purif Technol. 2015;149:16–23.
30. Lee H, Kim DS. Preparation and physical properties of wood/polypropylene/clay nanocomposites. J Appl Polym Sci. 2009;111:2769–76.
31. Radjenovic J, Petrovic M, Ventura F, Barcelo D. Rejection of pharmaceuticals in nanofiltration and reverse osmosis membrane drinking water treatment. Water Res. 2008;42:3601–10.
32. Rahmani K, Faramarzi MA, Mahvi AH, Gholami M, Esrafili A, Forootanfar H, et al. Elimination and detoxification of sulfathiazole and sulfamethoxazole assisted by laccase immobilized on porous silica beads. Int Biodeterior Biodegradation. 2015;97:107–14.
33. Baral SS, Das N, Ramulu TS, Sahoo SK, Das SN, Chaudhury GR. Removal of Cr (VI) by thermally activated weed Salvinia cucullata in a fixed-bed column. J Hazard Mater. 2009;161:1427–35.
34. Malkoc E, Nuhoglu Y, Dundar M. Adsorption of chromium (VI) on pomacean olive oil industry waste: batch and column studies. J Hazard Mater. 2006;138:142–51.
35. Ahmad AA, Hameed BH. Fixed-bed adsorption of reactive azo dye onto granular activated carbon prepared from waste. J Hazard Mater. 2010;175:298–303.
36. Song J, Zou W, Bian Y, Su F, Han R. Adsorption characteristics of methylene blue by peanut husk in batch and column modes. Desalination. 2011;265:119–25.
37. Aksu Z, Gönen F. Biosorption of phenol by immobilized activated sludge in a continuous packed bed: prediction of breakthrough curves. Process Biochem. 2004;39:599–613.
38. Han RP, Zou LN, Zhao X, Xu YF, Xu F, Li YL, et al. Characterization and properties of iron oxide-coated zeolite as adsorbent for removal of copper (II) from solution in fixed bed column. Chem Eng J. 2009;149:123–31.
39. Kumar PA, Chakraborty S. Fixed-bed column study for hexavalent chromium removal and recovery by short-chain polyaniline synthesized on jute fiber. J Hazard Mater. 2009;162:1086–98.

40. Vinodhini V, Das N. Packed bed column studies on Cr (VI) removal from tannery wastewater by neem sawdust. Desalination. 2010;264:9–14.
41. Hutchins RA. New simplified design of activated carbons systems. J Am Chem Eng. 1973;80:133–8.
42. Cooney DO. Adsorption Design for Wastewater Treatment. Boca Raton: CRC Press; 1998.
43. Thomas HC. Heterogeneous ion exchange in a flowing system. J Am Chem Soc. 1944;66:1466–664.
44. Yoon YH, Nelson JH. Application of gas adsorption kinetics I. A theoretical model for respirator cartridge service life Am Ind Hyg Assoc J. 1984;45:517–24.
45. Clark RM. Evaluating the cost and performance of field-scale granular activated carbon systems. Environ Sci Technol. 1987;21:573–80.
46. Rafati L, Ehrampoush MH, Rafati AA, Mokhtari M, Mahvi AH. Nanocomposite adsorbent based on β-cyclodextrin-PVP-clay for the removal of naproxen from aqueous solution: fixed-bed column and modeling studies. Desalin Water Treat. 2018;132:63–74.
47. Dehdashti B. Amin MM. Pourzamani H. Rafati L. Removal of atenolol from aqueous solutions by multiwalled carbon nanotubes modified with ozone: kinetic and equilibrium study. Wat Sci Tech. 2018; wst2018105.
48. Dehdashti B, Amin MM, Gholizadeh A, Miri M, Rafati L. Atenolol adsorption onto multi-walled carbon nanotubes modified by NaOCl and ultrasonic treatment; kinetic, isotherm, thermodynamic, and artificial neural network modeling. J Environ Health Sci Eng. 2019;17:1–13. https://doi.org/10.1007/s40201-019-00347-0.
49. Rafati L, Ehrampoush MH, Rafati AA, MokhtariA M, Mahvi AH. Removal of ibuprofen from aqueous solution by functionalized strong nano-clay composite adsorbent: kinetic and equilibrium isotherm studies. Int J Environ Sci Technol. 2018;15:513–24.
50. Rafati L, Ehrampoush MH, Rafati AA, MokhtariA M, Mahvi AH. Modeling of adsorption kinetic and equilibrium isotherms of naproxen onto functionalized nano-clay composite adsorbent. J Mol Liq. 2016;224:832–41.